

Design of a Novel Wheeled Tensegrity Robot: A Comparison of Tensegrity Concepts and a Prototype for Travelling Air Ducts

Francisco Carreño¹ and Mark A. Post²

Abstract. Efforts in the research of tensegrity structures applied to mobile robots have recently been focused on a purely tensegrity solution to all design requirements. Locomotion systems based on tensegrity structures are currently slow and complex to control. Although wheeled locomotion provides better efficiency over distances there is no literature available on the value of wheeled methods with respect to tensegrity designs, nor on how to transition from a tensegrity structure to a fixed structure in mobile robotics. This paper is the first part of a larger study that aims to combine the flexibility, light weight, and strength of a tensegrity structure with the efficiency and simple control of a wheeled locomotion system. It focuses on comparing different types of tensegrity structure for applicability to a mobile robot, and experimentally finding an appropriate transitional region from a tensegrity structure to a conventional fixed structure on mobile robots. It applies this transitional structure to what is, to the authors' knowledge, the design of the world's first wheeled-tensegrity mobile robot that has been designed with the goal of traversing air ducts.

Keywords. Bio-inspired Robots, Tensegrity, Wheeled Mobility

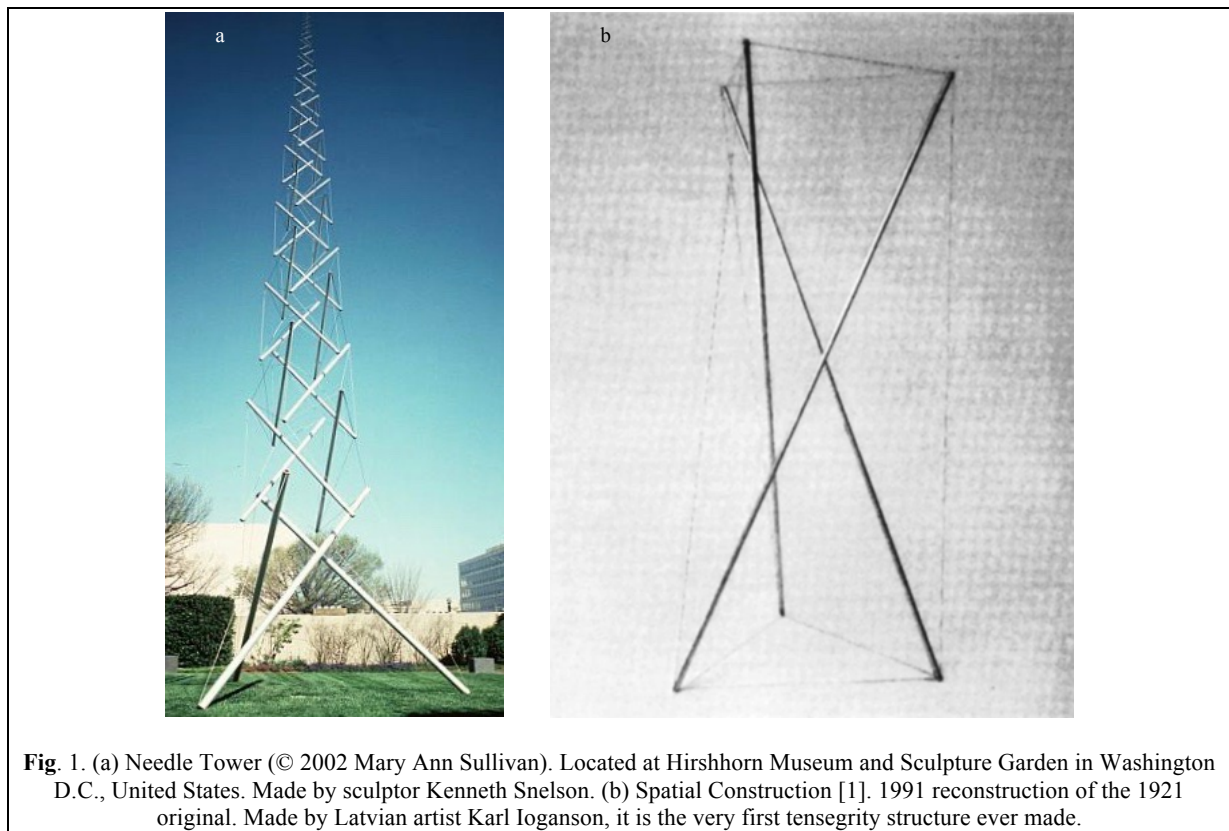
Introduction

A tensegrity structure is comprised of elastic elements and rigid elements that interact so the structure extends over a space larger than the space of its individual parts. The sum of the forces between all its parts is zero, therefore the structure is in equilibrium without the need of external forces. All elastic elements bear exclusively tensional force but not all tensional elements are elastic. The most spread-out use of rigid and elastic elements are struts and cables respectively. The "Needle Tower" (Fig. 1) is made of aluminium struts and steel cables. The struts are suspended in the air held only by cables. The structure rises with its internal energy compensating its potential energy. The first tensegrity structure was made by Latvian artist Karl Ioganson. It was shown in an exhibition in 1921 as part of his "Cold Structures" in the early Constructivism movement. Categorised at the time as a "Spatial Construction" (Fig. 1), the structure made is currently known as a 3-Strut Prism. Unfortunately, there was no further development of the novel structural principle [1]. Tensegrity structures were rediscovered by sculptor Kenneth Snelson who created "X-Piece" (also known as "Early X piece") in 1948 when he was still a student [2]. His professor, Buckminster Fuller, "asked Mr. Snelson to make a variation on 'Early X Piece,' which he later exhibited — without crediting his student — at an important exhibition at the Museum of Modern Art in 1959" [3]. They both ended up filing patents to claim authorship in 1959 (patent number 3.063.521 granted on 1962 to Fuller) and 1960 (patent number 3.169.611 granted in 1965 to Snelson). There is also a patent (number 1.377.290) granted to Emmerich in France in 1963 [4]. The word Tensegrity originated as the hyphenated word Tensile-Integrity Structure, coined by Fuller in his patent. Similarly, Snelson coined the name Continuous Tension, Discontinuous Compression Structures in his own patent.

¹ francisco.carreno.2016@uni.strath.ac.uk

² Correspondence: mark.post@strath.ac.uk

Department of Design, Manufacture, and Engineering Management, University of Strathclyde, 75 Montrose Street, Glasgow G1 1XJ, U.K.



Tensegrity Structures eventually expanded beyond art into engineering. Many studies have been done in statics, kinematics, dynamics, and biology. The main fields focused in tensegrity are civil engineering and robotics. The later have seen more than one thousand peer reviewed articles in the last 10 years. Research efforts in robotics span in all sub categories of study inside tensegrity: form-finding, kinematics, dynamics, control, and locomotion. Form-finding is the search for new topologies and morphologies of tensegrity structures. It also explores new methodologies to be used for the search itself. One of the sub areas of exploration is biotensegrity. This is the realm of tensegrity structures inspired by biology. Most research papers focus on implementing tensegrity to address all design specification requirements. Tensegrity and biotensegrity structures are light weight, strong, flexible, compliant, and distribute the loads to every single element. Yet, when it comes to locomotive efficiency, these structures do not perform as well. A man with a bicycle is capable of traveling much faster and farther than a man running in spite of using the same source of power: the muscles in the legs. This work aims to join the advantages of tensegrity structures and wheeled locomotion. As a practical application of this new concept, it presents a biotensegrity structure that is able to climb through ducting by pressing wheels against the walls. The tensegrity structure is to provide the robot structural integrity as well as control of direction. The tensegrity structure, therefore, will need to provide enough flexibility to allow the robot to turn right, left, up, down, and in any other intermediate direction so the robot can change its path into other duct branches.

This paper is the first part of the above-mentioned study into wheeled tensegrity robotics. It focuses on the transitional region from tensegrity to a standard fixed mobile frame for wheeled locomotion. To the authors' knowledge there is no formal research work done on this area. It firstly introduces criteria of evaluation for a transitional region. Secondly, it reviews of some of the available regular configurations of tensegrity structures as a preliminary study. Thirdly, it proposes new conceptual transitional regions to be validated later in the paper. Fourthly, it shows the design and prototype of a novel wheeled tensegrity mobile robot. Finally, it presents discussion and conclusions. As a representative problem that can be solved by a tensegrity-based wheeled robot, we have chosen the mechanical traversal and navigation of ducting networks. Ducting networks in buildings and industrial facilities can span and branch out in any direction in space. Most mobile robots are designed to travel only in a horizontal plane, and have difficulty turning in arbitrary directions in three dimensions. Robotic duct climbers are only able to travel in one line and maybe follow the duct mainstream through wide bends. They

currently do not have the ability to turn out of the duct into a branch. A robot able to transit through air ducts in houses and buildings will reduce time and number of personnel required as well as increasing flexibility and scope of work done. Due to the geometry and structural integrity of air ducts, flexibility and light weight are required key features. A hybrid wheeled tensegrity design would add speed and efficiency to the features of the robot. Basic work currently carried out in air ducts include inspection and maintenance. However, in the near future, home automation, pioneered by companies like Apple, Google, and Amazon, will require the installation of cable terminals to power automated air vents, and being able to access areas through complex duct networks will continue to become more relevant.

Literature review

Tensegrity structures have advantages and benefits. A list by Robert E. Skelton [5] includes: stability, efficiency, deployability, easy tuneability, reliability to be modelled, facilitation of high precision control, promoting integration of structure and control, and being inspired by biology. Other features proposed by Komendera [6] include reconfigurability, failure tolerance, simplicity of design, and ease of modelling.

Tensegrity is an ever-expanding field. Studies on tensegrity structures have been ‘widely carried out since 1970s, mainly about form-finding, static stability, and dynamic and control’ [7]. The work of finding new topologies and morphologies is called Form-Finding. This is a major subarea inside tensegrity robotics with several papers covering it. However, some researchers believe there are only a ‘few effective analytical methods for discovering tensegrity geometry’ [8]. Darrell Williamson and Robert E. Skelton [9] established a general class of tensegrity structures, defined the topological structure necessary to achieve tensegrity, and provided necessary and sufficient conditions for equilibrium. Motro [10] provided a description of ‘morphogenesis of tensegrity since earlier cells to present.’ Then he presented a numerical model to create more complex systems. Rieffel, Valero-Cuevas and Lipson [11] introduced an evolutionary algorithm which produces large tensegrity structures. They also demonstrated its efficacy and scalability relative to previous methods. They claim that those ‘techniques have produced the largest and most complex irregular tensegrities known in the field.’ On the other hand, Hernández and Mirats-Tur [12] did an important job to complement the above mentioned studies. They presented a method to detect and avoid ‘internal collisions between structure members and external collisions with the environment.’ Once there is a defined topology of a tensegrity structure and a initial stable placement, Micheletti and Williams [13] offered a ‘simpler approach for discovering the range of feasible geometries,’ or morphologies. Tensegrity is widely adopted by nature. Many researchers have taken inspiration from examples such as a vertebral column [14,15,16,17], a joint elbow [18,19], ant colonies [7], caterpillars [8] and fish [21] in order to produce new topologies called biotensegrity structures. They imitate their counterparts in nature and grasp some of the properties they possess.

After the topology and morphology are defined, mathematical models can be created. A static analysis review was carried out by Hernández and Mirats [4]. However, the dynamics were first studied by Motro, Najari, and Jouanna [22]. A model of tensegrity robotics based on Euler-Lagrange equations of motion was described by Komendera [6]. Mirats-Tur, Hernández, and Rovira [23] developed dynamic equations for a 3-bar tensegrity mobile robot. Cefalo and Mirats-Tur [24] proposed a new dynamic model for a class-1 tensegrity system based on quaternions. The use of quaternions eliminates problems of singularities and allow to perform more precise calculations and simulation as they do not need to use trigonometric functions for the representation of angles. This is a lesser developed area, there are only very few morphologies analytically analysed, being the most predominant, the 3-strut prism as in the works of Skelton and Oliveira [25].

When efficiency is mentioned as one of the features of tensegrity robots, it refers to this potential energy stored as tension inside the structure itself. However, this efficiency does not relate to locomotive movement. All research papers studying locomotion by means of tensegrity do not even measure efficiency in terms of distance covered over energy consumed. The only exception is Friesen [26], who stated that DuCTTv2 moves at 1.4cm/sec and Hustig [18] whose simulation of a robot moves at 3.8 cm/sec. Although there is no mention of energy consumption. Paul [27] introduced the idea of a legged robot based on tensegrity. Later, Böhm worked extensively and produced various papers (2012 - 2014) about locomotion by means of tensegrity mechanisms. His prototypes are capable of uniaxial rolling and movement in a plane with a combination of tip over and rolling. The approaches are not centred on locomotive efficiency and therefore there is no data related to velocity nor energy consumption. Rovira and Tur [28] derived dynamic equations of motion based on kinetic energy and potential energy expressions included in Euler-Lagrange equations. They simulated path trajectory including ground and friction into their model. Shibata, Saijyo, and Hirai [29] described the design of a tensegrity robot capable of crawling and proposed future designs that are able to jump. Bruce et al [30] developed a compliant and distributed tensegrity robotic platform for planetary exploration: SUPERball. The morphology of the robot is an icosahedral. It is a practical application

of tensegrity robotics that NASA sponsors. This paper does not focus on the locomotive part of the robot, only design. Sabelhaus [31] shows the construction aspect of SUPERball prototype. Friesen et.al. [32] developed another practical application, a tensegrity robot capable of climbing vertical ducts. Friesen's robot, called DuCTT (Duct Climbing Tetrahedral Tensegrity), comprises two tetrahedral frames connected by eight actuated cables. The robot holds to the duct by applying pressure against the wall with one linear actuator in each tetrahedron. It advances by moving one frame relative to the other. Researchers discuss in the paper the inverse kinematic control strategy used to actuate the robot. They point out that wheeled duct climbers can move quickly but 'have difficulty overcoming sharp corners or other irregularities' [32] and that the use of rigid joint legs require heavy actuators to achieve vertical ascent. Tests on this robot were included in an updated paper but the robot is still not able to turn into a branch of a duct. Friesen showed computer simulated work on NTRT (NASA Tensegrity Robotics Toolkit) developed by NASA to facilitate rapid design and control of tensegrity robots. Hustig [18], Mirletz [16], Lessard [20], SunSpiral [33], Bruce et.al. [30], and Sabelhaus [31] have also used NTRT. This software has been validated with prototypes.

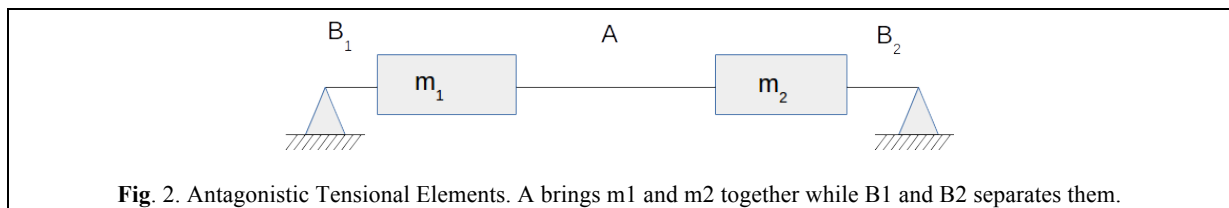
Criteria of Evaluation

Designing a hybrid tensegrity wheeled mobile robot, to the authors' knowledge, has never been attempted before. Therefore, some criteria of evaluation need to be established beforehand in order to be able to interpret the results of this study.

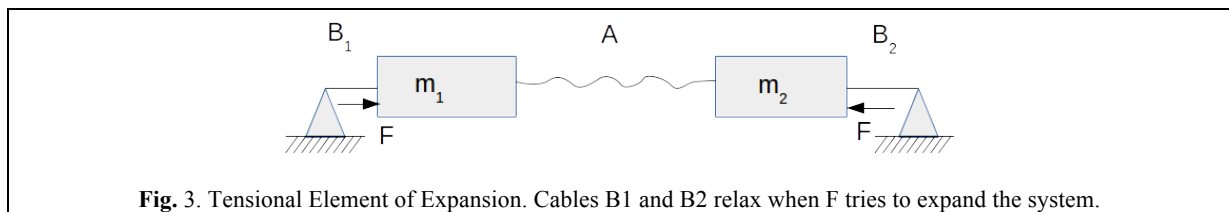
Antagonistic tensional elements

The first criteria developed was meant to classify Tensional Elements in two groups: elements that produce Contraction of the structure and elements that produce Expansion.

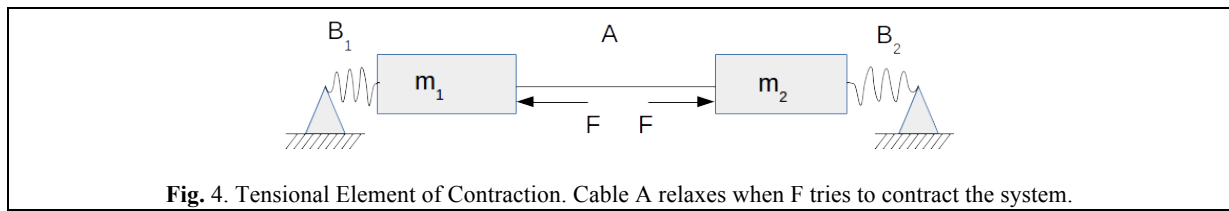
Consider the system shown in Fig. 2, comprised of two masses m_1 and m_2 joined by cable A and attached to fixed points by cables B_1 and B_2 at each side of the masses. The tension in cable A is T_a and the tension in cables B_1 and B_2 is T_b .



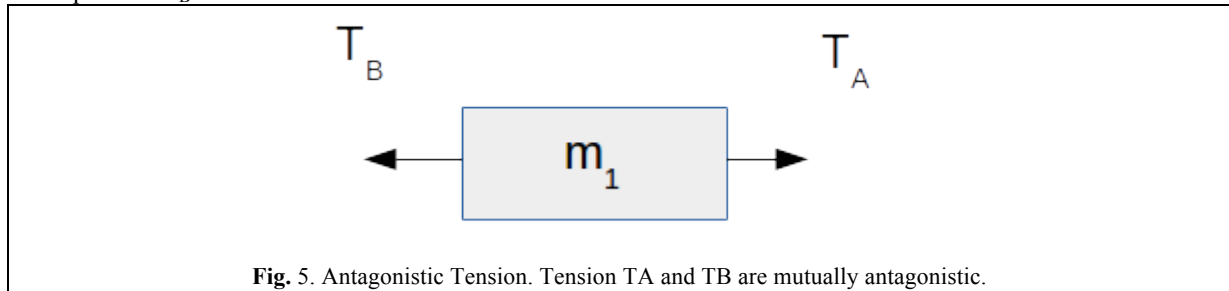
The first situation presented (Fig. 3) is the system affected by force F applied in the direction pointing towards the centre between the two masses. When this force is applied, tension in cable A is reduced by a magnitude F and tension in cables B_1 and B_2 is increased by a magnitude F . If the cables are elastic and force F big enough to stretch them, force F would bring masses m_1 and m_2 closer together. Force F is replacing cable A in bringing the masses together. Thus, it can be said that cable A brings masses m_1 and m_2 together. Tension in cable A is a tension of Contraction.



The second situation presented (Fig. 4) is the same initial system affected by a force F in the direction opposite to the centre between both masses. When this force is applied, tension in B_1 and B_2 is reduced by a magnitude F and tension in cable A is increased by a magnitude F . If the cables are elastic and force F big enough to stretch them, F would take masses m_1 and m_2 apart from each other. Force F is replacing cables B_1 and B_2 in separating masses m_1 and m_2 . Tension in cables B_1 and B_2 is a tension of Expansion.

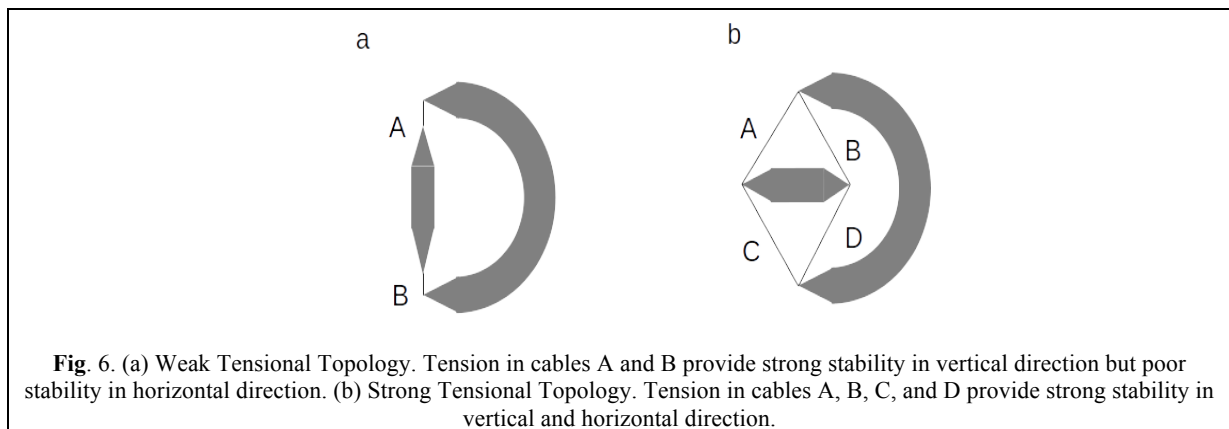


Mass m_1 is in stable equilibrium in the horizontal direction due to a Tension of Contraction T_A and a Tension of Expansion T_B .



Strong and weak tensional topology

The system topology shown in Fig. 6 (a) has strong stability in the vertical direction but poor stability in the horizontal direction. This is due to the fact that cables A and B are aligned with the vertical direction and perpendicular to the horizontal direction. The system topology shown in Fig. 6 (b) has strong stability in all directions in the plane. This is because cables A, B, C, and D have a projection in every direction of the plane. When designing a tensegrity system or a transitional region, this criterion has to be taken into consideration in order to have a stable system in all directions.



Review of Tensegrity Systems

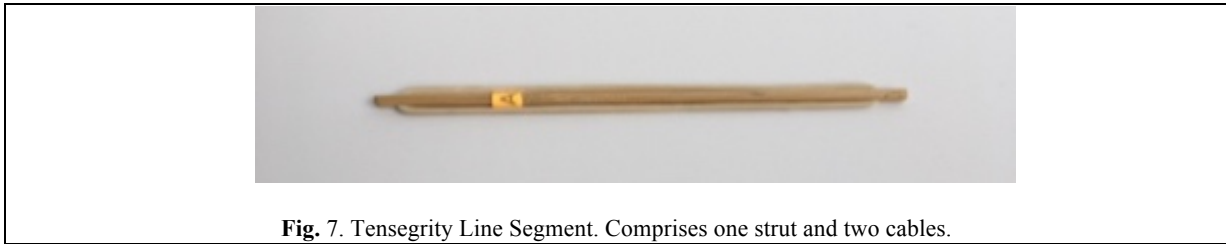
An extensive study of different topologies and morphologies was carried out as part of the research work needed to design a hybrid wheeled tensegrity mobile robot. It was an essential step in order to select the tensegrity structures that best fulfilled the design requirements. All tensegrity systems shown in this chapter were built by the author in order to gain a deep understanding of the capabilities, advantages and disadvantages of each of them relative to a duct traveling robot.

The area of tensegrity that studies the use of linear elements to form three-dimensional tensegrity structures is what the author calls Linear Tensegrity. This is where linear rigid elements, normally called struts or rods, and linear elastic elements, normally called strings or cables, are combined to form structures in two and three dimensions. Three-dimensional structures built with linear elements is the most common area of study in tensegrity. Planar tensegrity would also include the use of two-dimensional elements; this was not covered in this exploration due to the short time available.

The first half of this chapter studies the triangular prism. “Almost all tensegrities can be seen as variations on tensegrity prisms” [34]. It starts with a Line Segment and it builds up in steps until a Triangular Tensegrity Prism is achieved. The second half expands on the first one and explores other tensegrity systems.

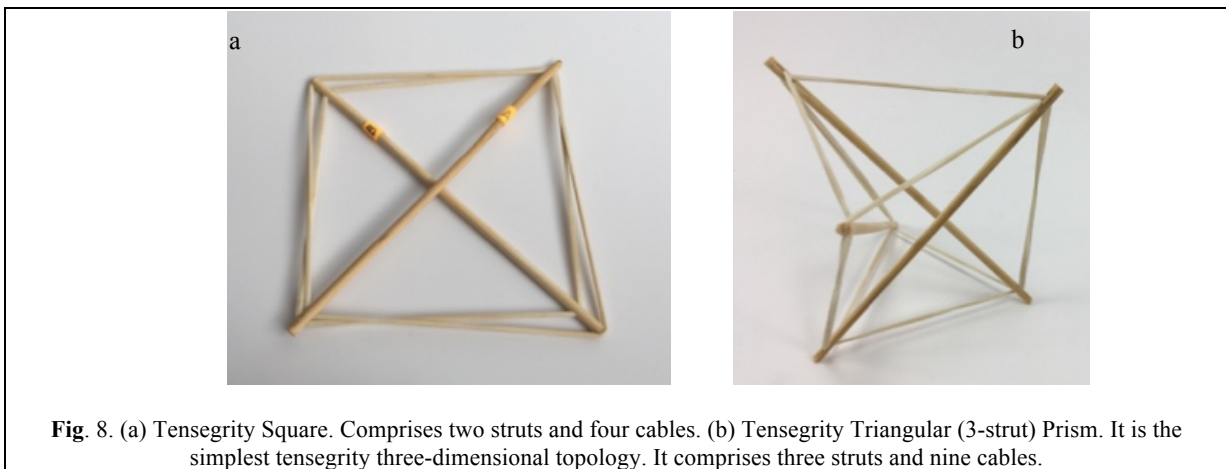
Line segment

Fig. 7 shows a tensegrity line segment composed of one strut and two cables at each side. This is the basic building block of most regular structures.



Square

A square is constructed by inserting a tensegrity segment into another one. Segment “B” is inserted in such a way that the ends of the strut are connected to the midpoint of the cables in segment “A”. Similarly, cables from segment “B” connect by the midpoint to the ends of the strut in segment “A”. The original cables in each segment are now considered split in two cables. Therefore, a square comprises two struts and four cables as shown in Fig. 8 (a). It should be noted that all elements can be considered to be in the same plane for practical reasons even though the struts are intersecting in the middle.



Triangular prism

A Triangular Prism is constructed by inserting a third tensegrity segment “C” into the previously seen square as shown in Fig. 8 (b). This is where the structure becomes three-dimensional.

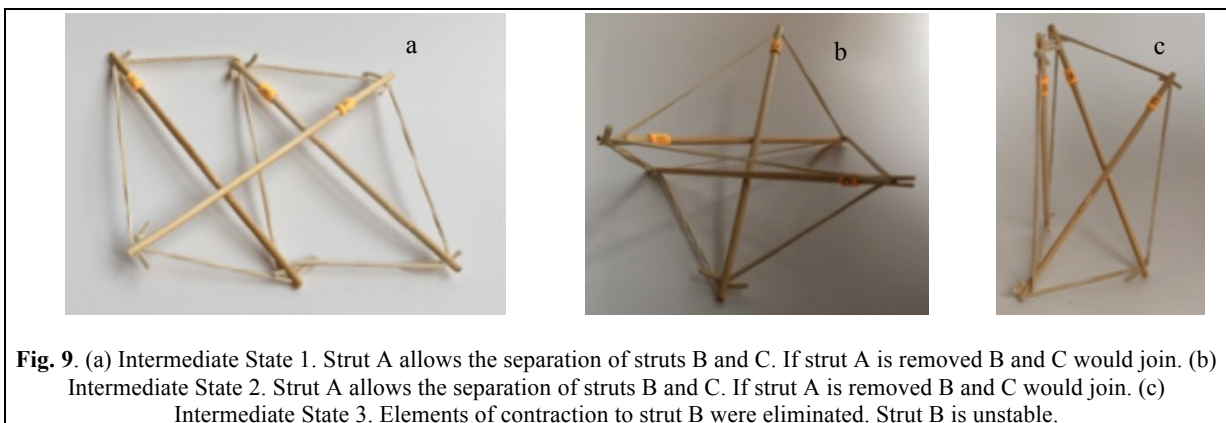
As part of this study, three intermediate structures between the tensegrity square and the triangular prism were devised. There is a particular nomenclature used in this analysis. The end of each strut is called a node. Each node is named according to the strut it belongs. At the top of the prism there are three nodes A_1 , B_1 , and C_1 . At the bottom of the prism there are three more nodes A_2 , B_2 , and C_2 . Cables are named in relation to the nodes. At the top, there are three horizontal cables forming a triangle A_1B_1 , B_1C_1 , and C_1A_1 . Notice that the order is not important; A_1B_1 and B_1A_1 is the same cable. There are three vertical cables A_1B_2 , B_1C_2 , and C_1A_2 . At the bottom, there are three more horizontal cables forming another triangle A_2B_2 , B_2C_2 , and C_2A_2 . Three intermediate state topologies can also be observed as follows.

Single plane: This intermediate state topology, Fig. 9 (a), is achieved by eliminating cables C_1A_1 and A_2B_2 . It can be seen that cables A_1B_1 , A_1B_2 , C_1A_2 and C_2A_2 are tension elements of expansion. They separate struts B and C. In the same way cables B_1C_1 , B_1C_2 , and B_2C_2 are tensional elements of contraction. Expansion elements

transmit the tension to a rigid element; strut A. Strut A is the inserted strut that allows separation of struts B and C. If strut A is removed Struts B and C would join. In this topology, two top horizontal cables, two bottom horizontal cables, and two vertical cables are elements of expansion. Similarly, one top horizontal cable, one bottom horizontal cable and one vertical cable are elements of contraction. If the topology is changed so now strut B is the inserted strut, it allows the separation of struts A and C, the same number of cables will be elements of expansion and contraction. Therefore, it is demonstrated that each cable in the prism topology is an element of expansion and contraction simultaneously.

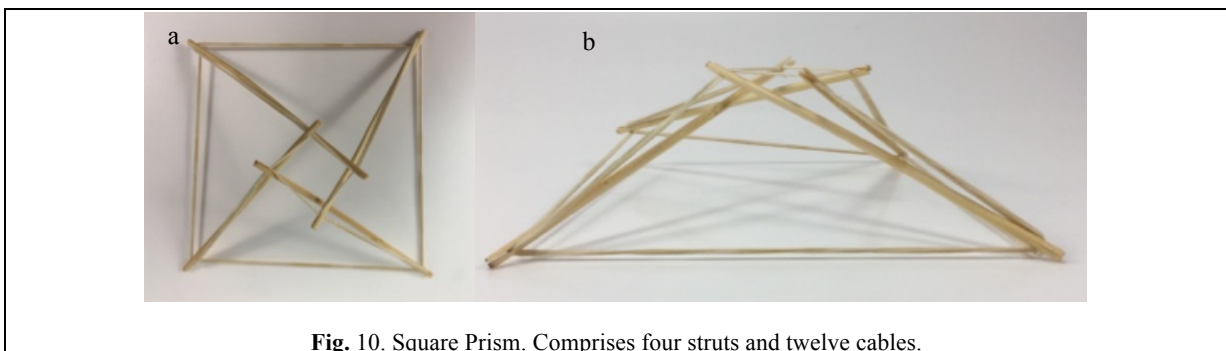
Dual plane with three intersecting struts: This intermediate state topology, Fig. 9 (b), is achieved by eliminating cables C1A1, A2B2 and adding cable C1B2. The structure collapses into two intersecting planes. The first plane is formed by struts A and B, second plane is formed by struts A and C. Strut A is the inserted strut separating struts B and C. The same case can be made to explain that all cables are elements of expansion and contraction simultaneously. Although in this topology one top horizontal cable, one bottom horizontal cable, and two vertical cables are elements of expansion.

Dual plane with two intersecting struts: This intermediate state topology, Fig. 9 (c), is achieved by eliminating cables B1C1 and A2B2. The prism is broken into two planes. The first plane made by struts A and C and the second by strut B. This state is unstable as strut B can rotate along its connected points to strut A and C. The eliminated cables are elements of contraction. The remaining cables attached to strut B are elements of expansion. Thus, it can be appreciated how they interact to keep strut B stable.



Square prism

A square prism is comprised of four struts and twelve cables. Fig. 10 (a) shows a better adaptability to square ducting where each strut could be pressed against each corner of the square section in the duct. The morphology shown in Fig. 10(b) has the top square with larger dimensions than the bottom square. This could be beneficial for expanding a narrow axle into a much bigger structure or as a joint between a square bar and another tensegrity structure.



Octagonal prism

Comprised of eight struts and twenty-four cables, the octagonal prism is also well suited for square ducting and is shown in Fig. 11 (a). Two struts could press into each wall of the duct. By expanding and contracting one of the octagons, the robot could adapt to different duct sizes such as in Fig. 11 (b). The end of the struts could be attached to wheels in order to support the structure inside the duct. This topology could also be used as a vacuuming tool. If the struts are made of piping and hooked to hoses converging into one hose, this tool could vacuum the walls of different sizes of square duct.

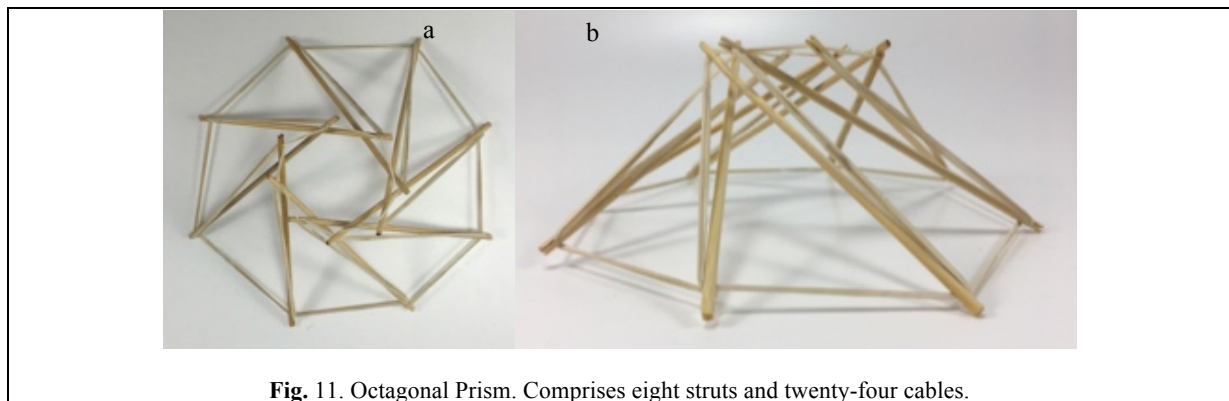


Fig. 11. Octagonal Prism. Comprised eight struts and twenty-four cables.

Icosahedron

The Expanded Octahedron or Icosahedron, Fig. 12 (a) has six struts and twenty-four cables. The morphology of this topology can be changed into a truncated tetrahedral by simply changing the length of the cables. If the parallel struts of the Icosahedron are brought together it forms an octahedron and therefore has the name of Expanded Octahedron.

This structure resembles a ball when all struts are the same length. In fact, NASA is developing a robot with this same topology that is capable of rolling as method of locomotion [31]. In relation to a duct travelling robot, this could probably be useful as a joint.

Octahedron

Formed by joining the parallel struts of the Icosahedron together, Fig. 12 (b). This morphology could also be used as an intermediate state between a tensegrity and a solid. Although this is not as flexible as other tensegrities as it has all struts joined in the centre.

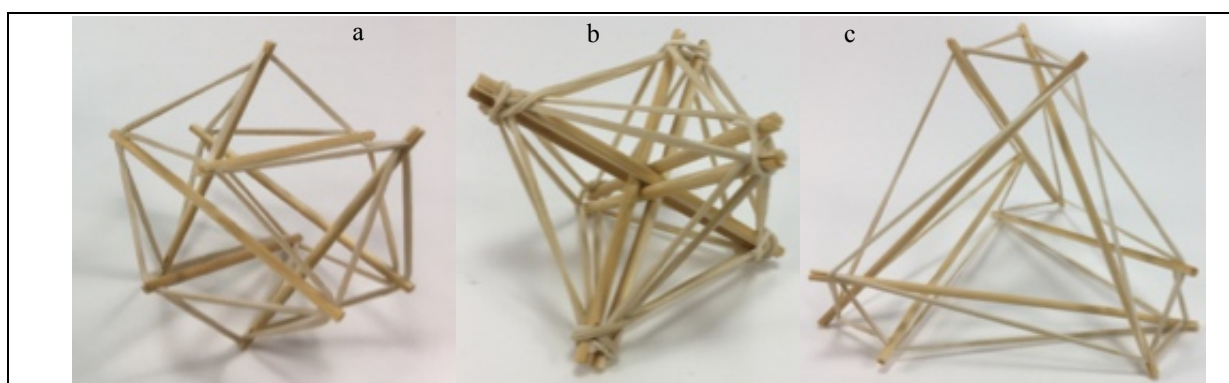


Fig. 12. (a) Icosahedron. Comprised six struts and twenty-four cables. (b) Octahedron. Comprised six struts and twenty-four cables. (c) Truncated Tetrahedral. Comprised six struts and twenty-four cables.

Truncated morphologies

The Truncated Tetrahedral, Fig. 12 (c), can be made by varying the length of the cables in the Icosahedron. Both are two morphologies of the same topology. Although this Tetrahedral was built with segments made one strut and two cables, it can also be constructed with segments made of one strut and one cable. One interesting property of this morphology is that it can be made into other geometrical form by adding struts following the same pattern.

A Truncated Cube, Fig. 13 (a), can be made with 12 struts and 33 cables. When the ends of the struts on each side of the cube are joined closer together a different morphology comprised of four intersecting triangles is made as in Fig. 13 (b) with these triangles indicated.

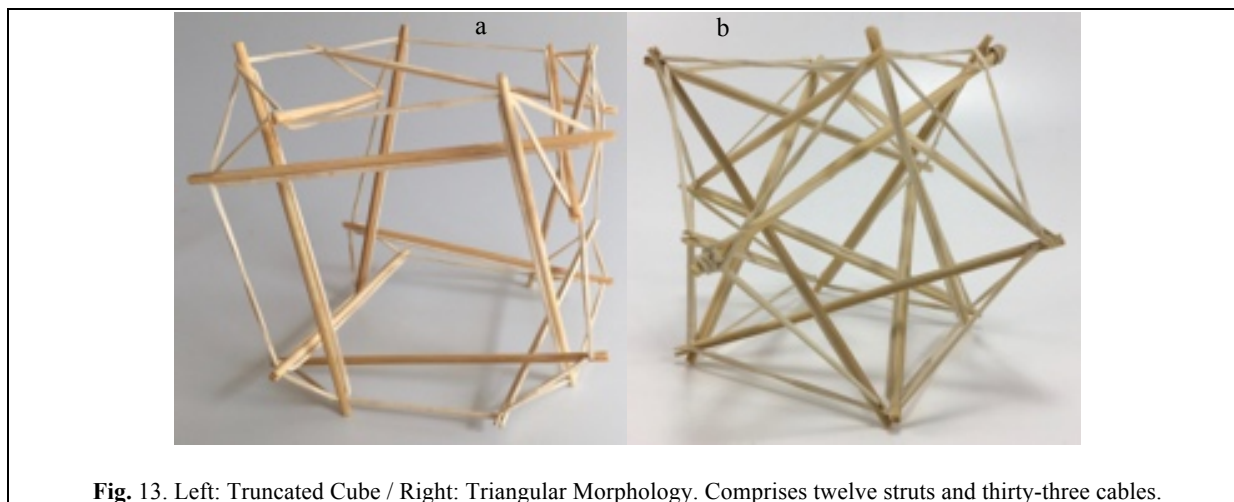


Fig. 13. Left: Truncated Cube / Right: Triangular Morphology. Comprises twelve struts and thirty-three cables.

Following the same pattern, a Truncated Dodecahedral, Fig. 14, can be built with 30 struts and 90 cables and having five-sided faces. All these structures behave essentially as a ball and are not of practical use for the purposes of the duct-climbing robot in this paper.



Fig. 14. Truncated Dodecahedral. Comprises thirty struts and ninety cables.

Spiral vertebral mast

This structure is built in stages. Each stage has three struts. The second stage attaches to the cable midpoint of the first stage. The orientation of each stage changes, if the first stage is oriented clockwise, the second stage is oriented counter clockwise. This structure, designed by Tom Flemons, can be built to be as long as desired following the same pattern. At its minimal topology, it only has tensile elements of contraction as shown in Fig. 15 (a). This is why in a state of equilibrium, with no other external forces, it looks shrunk in its radial direction. It does not take a great volume in space. The tension forces are almost aligned axially which creates a weak tensional morphology in the radial direction. This could be corrected by adding antagonistic tensional elements as shown in Fig. 15 (b). This structure can be totally collapsed along its axial direction as shown in Fig. 15 (c) and will recover its original form when the external force applied is eliminated. The structure can be built with three or more struts in each state following the same pattern.

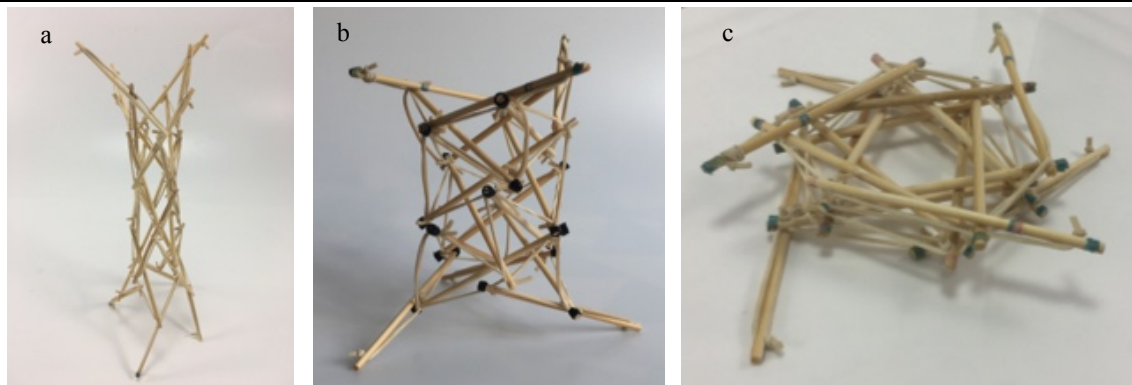


Fig. 15. Spiral Tensegrity Mast. (a) Minimal Topology. (b) Antagonistic Tensional Topology. (c) Collapsed State. Achieved by placing a glass on top of the mast.

Tetrahedral vertebral mast

This mast comprises rigid elements joined together by eight cables as shown in Fig. 16 (a). Each rigid element comprises four struts rigidly joined together as indicated in the centre of the element as shown in Fig. 16 (b). This structure, also designed by artist Tom Flemons, can be built with as many stages as needed. It is possible that the rigid tetrahedral can generate momentum forces at the centre of the rigid elements. This is something that could be further evaluated. With the materials used in these models and the prototypes, the rigid element did not fail at its core. It was more likely to break at the rubber band wedge. This structure, in a way, is a simplification of the Vertebral Column shown in Fig. 16 (c); each rigid element is one vertebra. In this analogy, there is no Vertebral body and it is replaced by a strut as if the vertebra had two Spinous Processes. The two Transverse Processes are replaced by two struts as well.

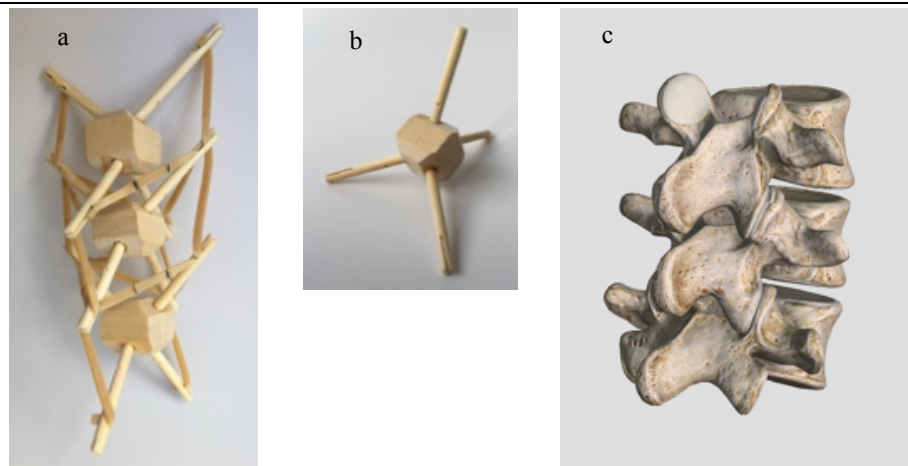


Fig. 16. Tetrahedral Vertebral Mast. (a) Three stages fully assembled. (b) One isolated stage. (c) Animation of part of Vertebral Column [35]

There is no representation for any of the four Articular Processes. They are omitted in this model which is one of the biggest differences. The forces produced by the Vertebral body, and Articular Processes are being replaced by horizontal cables. The connections between the Transverse Processes in each vertebra are identically substituted by vertical cables. The connections between the Spinous Processes are also substituted by vertical cables. This structure is one of the few examples in which the element of contraction and expansion are well defined. Horizontal cables are exclusively tensional elements of expansion while vertical cables are exclusively tensional elements of contraction.

In summary, both topologies, Spiral Vertebral Mast and Tetrahedral Vertebral Mast, present similar characteristics that are greatly beneficial for a duct traveller robot:

- Vectorial shape. It can point to a determinate direction and it has a clear axial direction.

- Built in stages. They can be added or subtracted to increase or reduce the robot length.
- Radial degrees of freedom. It allows the structure to Yaw and Pitch in an unlimited number of directions. It is virtually a universal joint.
- Axial degree of freedom. It allows the structure to Roll.
- Axial displacement. The structure can extend and contract axially.
- Pattern repeated in the axial direction. Easy to manufacture and repair.

Transitional Regions

There are studies, like Motro [36], that address the problem of joining together various tensegrity structures to form more complex and bigger ones. However, to the authors' knowledge, there are no studies that address the problem of joining together a tensegrity structure with a fixed one. Therefore, in order to connect a tensegrity structure with a traditional mobile fixed structure, a new methodology will need to be developed. The following is a series of concepts that need to be formalised in the area of tensegrity and robotics.

Localised tensegrity

Typical tensegrity structures have cables attached to struts at the ends of the strut. It should be noticed that this is common to see but not a requirement that defines a tensegrity system. This arrangement is so spread among the research community that limits the creativity of new topologies.

When observing the musculoskeletal systems of animals, it can be noticed that groups of muscles and tendons are localised into regions (i.e. shoulders, hips). Bones are the only elements to transcend those limits. So it can be observed that the humerus extends beyond the shoulder and at the same time the muscles in the shoulder area are located on one end of the humerus and do not extend up to the other end of it. In this case it can be considered that the rigid body acts as the transitional region between two localised tensegrity regions.

There are few exceptions to this paradigm that are starting to appear. Hustig [18] did apply the concept of Localised Tensegrity in one of the iterations of his MountainGoat design. Figure 17 shows two versions of his design, one tensegrity system in (a) and two localised tensegrity regions in (b): the main body on top and a foot at the bottom. As seen in the previous example, this concept can open the door to new more complex tensegrity systems comprised of multiple Localised Tensegrity Regions. Each of them can be designed to perform specific functions in the entire structure.

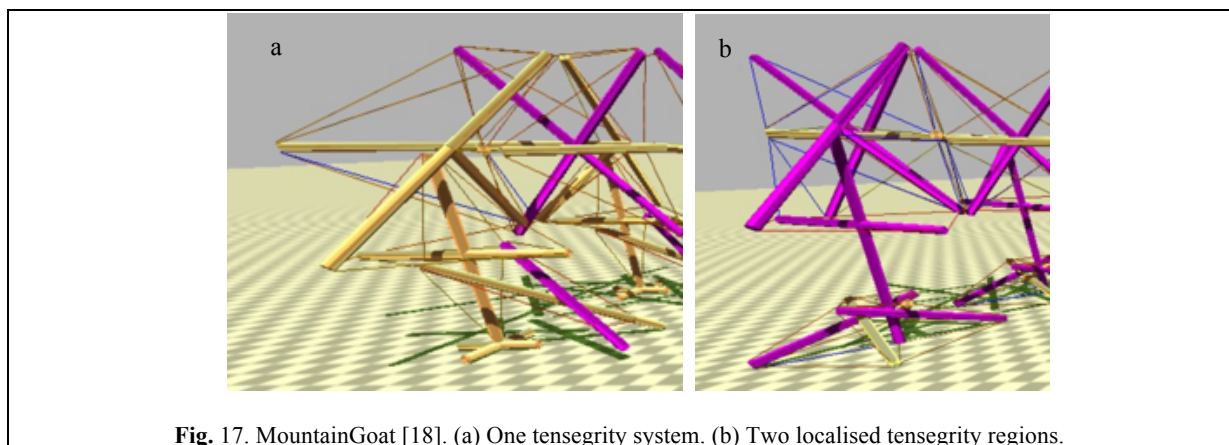


Fig. 17. MountainGoat [18]. (a) One tensegrity system. (b) Two localised tensegrity regions.

Hard transitional region

It is a transition made exclusively of rigid elements. This type of transition is linked to the concept of Semi-Continuation described in the following part.

Soft transitional region

It is a transition made exclusively of elastic elements. To properly work, it needs to have an Antagonistic Tensional Setting: Elements of Contraction and Elements of Expansion.

Fulfilled pattern

The Lumbar Vertebrae are connected among themselves by three surfaces. One located at the Vertebral Body and two at the Articular Process. In total, a Lumbar Vertebrae has six joints: three at the top and three at the bottom. This means that the Fifth Lumbar Vertebra, the last one at the bottom, needs three surfaces of connection as well when joining the Sacrum. The Sacrum at birth is composed of five separate sacral vertebrae. Postnatally they fuse to form a single bone that is flattened anteroposteriorly and has a triangular shape when viewed from the front [37].

This is where the principle of Fulfilled Pattern takes place. When connecting a chain of rigid elements of the same morphology to another element of different morphology, the morphology of the first needs to be satisfied by the second. That is the Sacrum needs to have the same top three connecting surfaces to receive the bottom three connecting surfaces of the Fifth Lumbar Vertebra. Figure 18 shows how the Sacrum follows the same pattern.

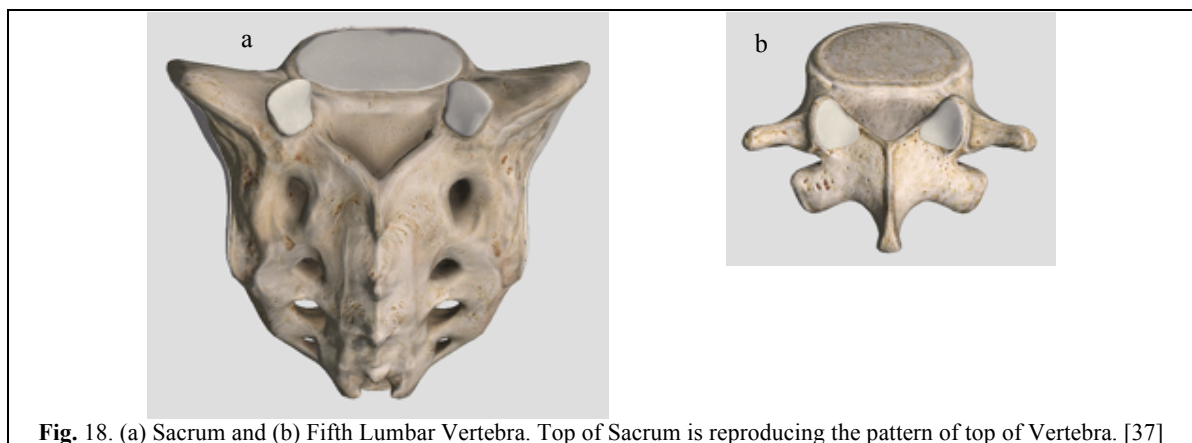


Fig. 18. (a) Sacrum and (b) Fifth Lumbar Vertebra. Top of Sacrum is reproducing the pattern of top of Vertebra. [37]

Unfulfilled pattern

This concept can be observed in the connection of the Scapula to the Axial Skeleton in the Musculoskeletal System of the Human Body. The Scapula attaches to the Axial Skeleton with only Soft Tissue. The scapula (shoulder blade) is a flat, triangular bone located along the posterior aspect of the thoracic cage. Seventeen muscles attach to the scapula; therefore, this bone is usually resistant to fractures [35]. Since the attachment of the scapula to the Axial Skeleton is exclusively made by muscles there is no requirement to imitate the form of the adjacent structure as in the previous case. Those seventeen muscles are arranged in a way that allows the body to (1) set an equilibrium state in which the scapula is at a particular location and (2) move the scapula around in a controlled way. This is a more complex joint to design. It certainly needs to be design with antagonistic tensional elements and strong tensional topology.

Robot Design and Prototyping

This research work was mainly exploratory as it was set to design the first wheeled tensegrity mobile robot. Due to this circumstances it was best to design by building prototypes in an iterative process. When using tensegrity structures to design mobiles robots, designers face the following challenges [4]:

- Static analysis of tensegrity structures: Find a stable configuration from a given topology or even design new topologies to achieve some desired results.
 - Form-finding methods
 - Static behaviour of tensegrity.
 - Rigidity and stability.
- Dynamics and control of tensegrity: Plan trajectories and motions taking into account the advantages that tensegrity structures offer.
 - Traditional path planning algorithms.
 - Dynamic characterisation of tensegrity structures.
 - Node trajectory planning.

Work environment

The design was focused on achieving two main requirements for this robot: (1) unprecedented flexibility for a duct travelling robot and (2) unprecedented locomotive performance for a tensegrity robot. With this in mind, an evaluation of the current geometric characteristics of air ducting is needed. Most common rectangular air ducts

range from 100mm x 200mm to 150mm x 300mm and circular ducts, from Ø100mm to Ø200mm in households. The layout of ducts is mainly in a horizontal plane with turns right and left. There are also branches that go upward and downward. There are two requirements here: (1) a robot must adapt to the range of ducting sizes and (2) the robot must be flexible enough to turn not only left and right but also up and down.

While requirement number one have already been solved by several designs, requirement number two has not. There are no robots in the market, to the authors' knowledge, that can turn in all four directions and is able to vertically climb. Therefore, requirement number two is the main focus of the design in this paper. This process has begun with a selection of the main tensegrity structure of the robot. It was followed by the design of a transition from tensegrity elements to a solid body. Finally, a model for the robot was made.

Structure

Taking advantage of the flexibility of tensegrity structures to allow the robot to turn in every direction was the main requirement of this section. All tensegrity structures are flexible but not all of them have special flexibility in particular directions. Most of the structures tend to be omnidirectional and resemble the shape of a sphere.

However, there are two topologies that fit the needs of a duct traveller robot: The Spiral Vertebral Mast and Tetrahedral Vertebral Mast. They were chosen for the reasons explained in section 5. There is a slight modification to the original Spiral Mast: the structure constructed for the prototype was built with four struts on each stage for two reasons: (1) the robot will mainly turn up, down, right, and left, and (2) the robot fixed rigid body is a square bar. Therefore, four struts accommodate the geometric requirements better.

Transitional region

Initially one prototype was made for each structure following the criteria of a Hard Transitional Region and Fulfilled Pattern. For the tetrahedral vertebral mast (also called tensegrity spine), it was necessary to build all four struts and not only two as it was originally thought as shown in Fig. 19 (b). For the spiral tensegrity mast (also called tensegrity mast), the construction process was carried out by placing the entire tensegrity mast next to the square bar, applying an external force to the four struts at the end of the mast until they touch the bar and gluing them while keeping the position they naturally acquired. When the glue dried the four struts did not belong to the tensegrity structure anymore but to the square bar as shown in Fig. 19 (a).

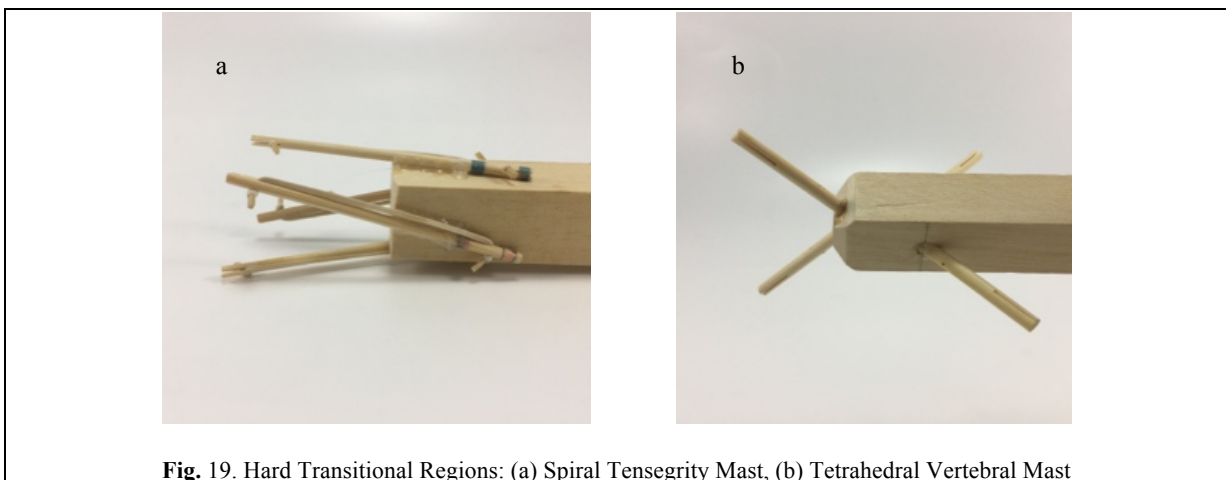


Fig. 19. Hard Transitional Regions: (a) Spiral Tensegrity Mast, (b) Tetrahedral Vertebral Mast

As can be seen in Fig. 20, both transitional regions imitate the pattern of the tensegrity structure (fulfilled pattern). Both tensegrities are capable of turning 90° in any radial direction, as well as rotating and translating in the axial direction. This concept worked well with the tensegrity spine shown in Fig. 20 (a). It did not change any of the properties of the original tensegrity structure. Axial translation, radial translation, axial rotation and radial rotation remained the same. This design is acceptable and no further development is needed for this structure. However, this concept did not work as well with the tensegrity mast shown in Fig. 20 (b). It added rigidity to the original tensegrity structure and changed its mechanical properties. So much so that the structure was not able to axially collapse anymore. Collapsibility is not really a requirement for this design, so the prototype was acceptable as well.

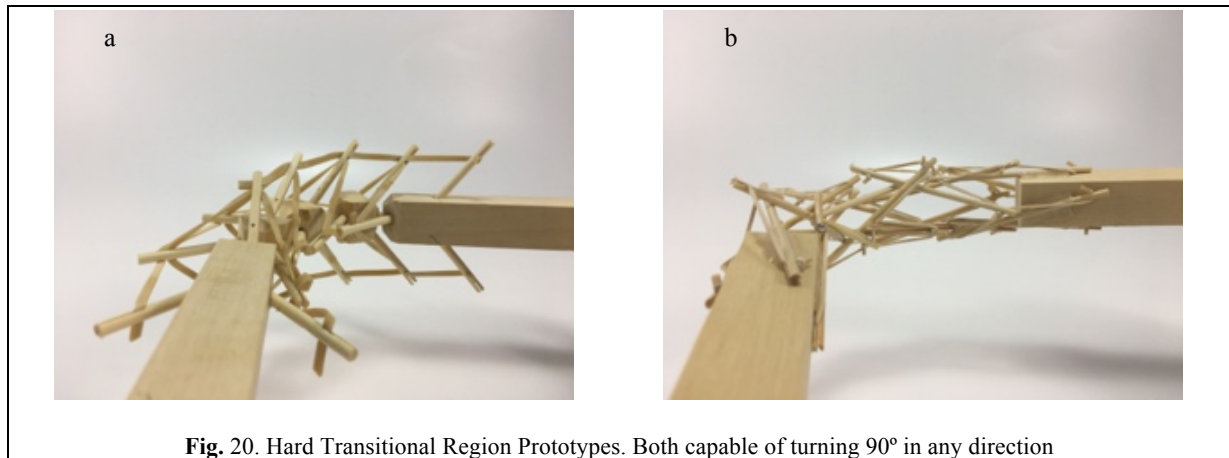


Fig. 20. Hard Transitional Region Prototypes. Both capable of turning 90° in any direction

Two more prototypes of the spiral mast transitional region were made following the concept of soft transitional regions and unfulfilled patterns. However, the design was not tensional-antagonistic and it had a weak tensional morphology. Therefore, the structure was unstable. More development would be needed to achieve both requirements in future prototyping iterations.

Final model

The final prototype is the first wheeled tensegrity mobile robot ever built to the authors' knowledge. It was made with readily available and recycled parts in the design laboratory at the University of Strathclyde. The final design comprises two motorised modules and one non-motorised module which are shown in Fig. 21. Motorised modules have two wheels of Ø44mm at the bottom and one wheel of Ø23mm at the top. The top wheel presses against the wall of the ducting. The motor runs on 4.5V 0.41A at 4900rpm. Overall dimensions are 110mm x 58mm x 80mm. The non-motorised module has 4 wheels of Ø30mm distributed in two pairs that press against the duct for stability. Overall dimensions are 75mm x 62mm x 74mm. All three modules connect to the tensegrity by a hard transitional region and fulfilled pattern.

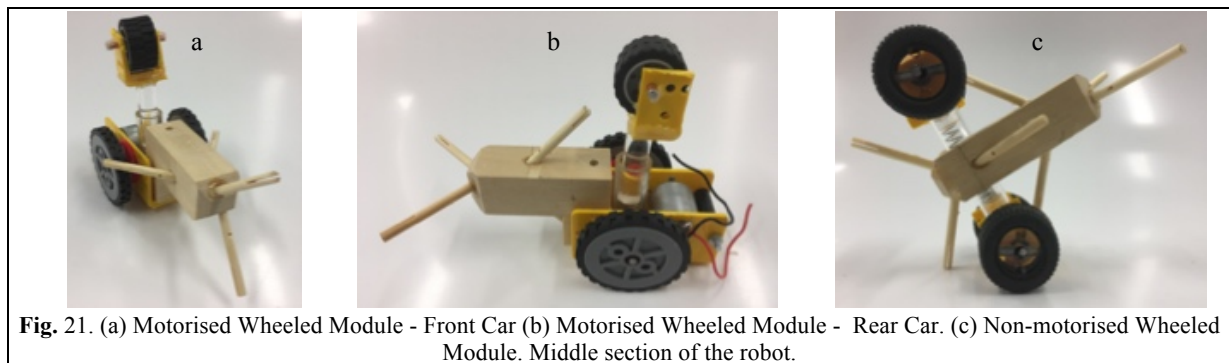


Fig. 21. (a) Motorised Wheeled Module - Front Car (b) Motorised Wheeled Module - Rear Car. (c) Non-motorised Wheeled Module. Middle section of the robot.

The robot has five sections. The first one is the front car, the second one is the front tetrahedral vertebral mast, the third one is the middle car, the fourth one is rear tetrahedral vertebral mast, and the fifth one is the rear car, as shown in Fig. 22. Overall dimensions are 500mm x 62mm x 80mm. Total weight is 303g. A pipe environment was built to assess the robot's flexibility in operation. The model was capable of turning in horizontal and vertical planes inside the pipe as shown in Fig. 23. This kind of flexibility would require a high level of mechanical complexity in a conventional mobile robot. This robot was built in a very short amount of time with low cost materials.



Fig. 22. Wheeled Tensegrity Mobile Robot (WTMR). It comprises three rigid structures and two tensegrity structures.

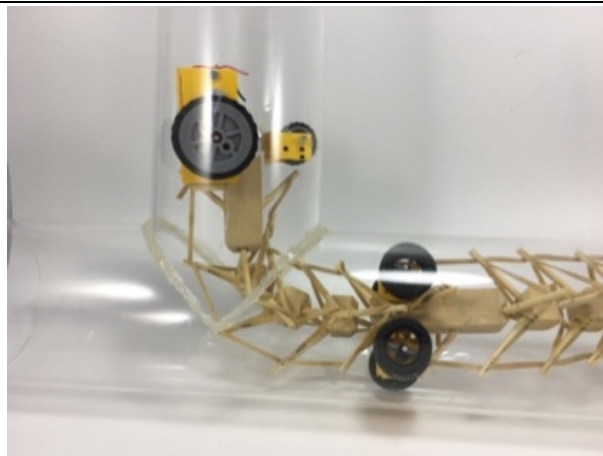


Fig. 23. Wheeled Tensegrity Mobile Robot (WTMR) turning inside a pipe.

Physical Testing and Discussion

Rubber characterisation

Three tests were performed to analyse the mechanical characteristics of the rubber band used to build the prototypes. In all three, 100mm rubber band samples were used. The results showed that the mechanical properties of the rubber band deteriorated after a 20% displacement. Therefore, in order to have consistent results any deformation further than 20% was avoided. There was no noticeable linear pattern in the 20% deformation region, therefore a simple linear formula was avoided and the tension in the cable was determined from interpolation of the experimental results obtained in Fig. 24.

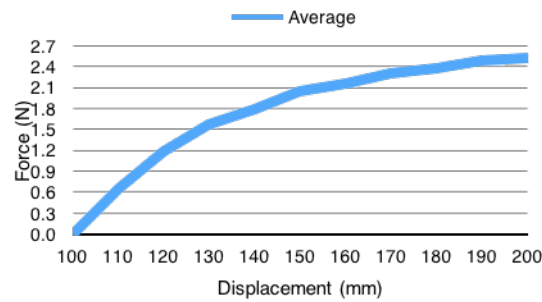


Fig. 24. Rubber Band Test 3: Force vs Displacement. Test of 100mm rubber band. Average of 15 times per displacement. Elastic zone determined was within 120mm.

Tensegrity spine

The first set of tests were performed on three stages of the tensegrity spine (T1, T2, T3). The purpose of the tests was to find the tension supported by each cable and how much tension was needed to bend the spine when unloaded and when linked to a load. The tensegrity spine was made out of soft wood and bamboo sticks. Rubber bands were used as cables. Custom made rubber band loops were made with specific lengths (gluing together the ends) to be used as horizontal cables. The test consisted on measuring final length of 10mm marks made on each cable. By measuring the displacement, the tension on the cables could be approximated. Tension in the actuator was also measured.

Test 1. Rubber band loops made were 120mm long which means that each horizontal cable was 30mm long. Each vertical cable was also 30mm long. Displacement was measured with no actuation and no loads acting upon the structure. Cable T3H4 (horizontal cable on the back left of rigid element T3) was the most loaded, showing a displacement of 70%. It should be noted that this cable shows more tension due to the fact that the rigid elements are not perfectly symmetric. In later tests, this was compensated by slightly varying the length of the cables. Table 1 shows the percentage displacement in all rubber band cables. Such high displacements over 20% greatly reduce the consistency of the data obtained. Therefore, the length of all horizontal cables had to be increased. Table 2 shows the calculation of the final length of rubber band loop T3H that comprise cables T3H1, 2, 3, and 4. The next test required a new set of rubber band loops that work under 20% displacement.

Table 1. Tensegrity Spine Test 1. Percentage of displacement in each horizontal (H) and vertical (V) cables.

T2H1	30%	T3H1	35%	T1V1	10%	T2V1	20%
T2H2	40%	T3H2	50%	T1V2	10%	T2V2	15%
T2H3	30%	T3H3	50%	T3V3	15%	T2V3	10%
T2H4	45%	T3H4	70%	T3V4	15%	T2V4	20%

Table 2. Final Length of Rubber Band Loop T3H (mm). Calculated by adding displacements of T3H1, T3H2, T3H3, T3H4.

	Disp.	Initial length	Final Length
T3H1	35%	30	40.5
T3H2	50%	30	45
T3H3	70%	30	51
T3H4	50%	30	45
Total			182

Test 2. For this test, 152mm long Rubber bands were prepared. With a displacement of 20% the final length of the band was 182mm which covered the displacement seen in Test 1. Test 2 comprises a set of 6 different runs. The first two runs were done with no actuation nor load. Runs 3 to 6 have an actuator cable to bend the tensegrity spine up, down, left, and right. The tension in this cable was measured as well. Run 1 showed cable T3H3 with a displacement of 25%. The length of the cable was slightly adjusted before the second run. Run 2 shows that this displacement was reduced to less than 20%; right under operational range. The next runs were under actuation to bend the tensegrity spine in four different directions. Two major displacements have been highlighted in Table 3. From these two, run 4 shows the most extreme results. Vertical cables are within limits. The measurements and calculations to get the final length of rubber band loop T3H are shown in Table 2. Total length of T3H was calculated to be 193mm. Therefore, a new length for the loops needed to be used.

Table 3. Tensegrity Spine Test 2. Runs 1 and 2 have no actuation. Runs 3 to 6 have a cable actuator in order to bend the tensegrity spine up, down, left, and right. Tension of actuator T(N).

	1	2	3	4	5	6
			Up	Down	Left	Right
T2H1	10%	10%	20%	10%	20%	10%
T2H2	10%	10%	25%	15%	10%	20%
T2H3	10%	10%	8%	20%	0%	30%
T2H4	10%	10%	30%	30%	40%	20%
T3H1	10%	10%	30%	20%	25%	10%
T3H2	19%	15%	30%	20%	20%	30%
T3H3	25%	18%	20%	40%	10%	35%
T3H4	15%	18%	20%	30%	30%	10%
T1V1	5%	5%	0%	0%	0%	10%
T1V2	0%	0%	0%	0%	10%	0%
T2V1	20%	20%	10%	0%	0%	10%
T2V2	10%	10%	0%	0%	10%	0%
T2V3	10%	10%	0%	10%	0%	0%
T2V4	11%	11%	20%	0%	10%	5%
T3V3	10%	10%	0%	10%	0%	0%
T3V4	9%	9%	10%	0%	0%	0%
T	0	0	1.9	1.7	2.1	2.1

Test 3. Rubber band loops of 160mm were prepared for the third test. With a displacement of 20% a final length of 192 will be covered. The first 2 runs were made with no load and no actuation just to compensate for any peaks in tension in any of the cables. Indeed, some of the cables needed adjustment like T2H4 and T3H4 that were adjusted from 16% to 6% and 13% to 8% respectively. Runs 3 to 6 were performed with actuation and no load. All displacements were under 20% this time. Runs 7 to 10 were performed with the front car (94g) attached to the tensegrity spine. The results in Table 4 show a maximum displacement of 27% on cable T3H4 and a maximum actuation force of 12.4N.

Table 4. Tension in Horizontal Cables (N). Interpolation of tension based on displacement of rubber

	3	4	5	6
T2H1	0.96	0.06	0.9	0.42
T2H2	1.2	0.3	0.48	1.2
T2H3	0.48	1.2	0.48	1.2
T2H4	0.78	0.72	0.72	0.72
T3H1	1.02	0.36	1.02	0.36
T3H2	1.08	0.54	0.66	1.2
T3H3	0.78	0.78	0.6	1.2
T3H4	0.78	0.96	1.08	0.66

The use of rubber bands as a tension medium proved to be a limiting factor since the beginning of the experiments due to the quick degradation of its mechanical properties (Fig. 24). Nevertheless, it was a quick and cheap method of prototyping and some useful information could still be drawn from the tests. It was determined that the working zone for this rubber band was under 20% displacement and 1.2N of force (Fig. 24). With these conditions, it was determined in Test 2 an optimal length of 160mm for horizontal rubber band loops and 30mm for vertical rubber bands. However, Test 3 demonstrated that the Front Car, weighing 94g, was too big a load for the rubber bands. Additionally, it was noticed that in the runs with the 94g load the tensegrity rigid elements started touching each other. This meant the tensegrity stopped behaving as such; cables in the tensegrity structure did not bear all loads anymore. The structure was overwhelmed by the load. Runs 3 to 6 in Test 3 can be used as an approximated method to calculate the loads on each cable based on the tension in the actuator, displacement, and Fig. 24.

Conclusions

The very first wheeled tensegrity mobile robot was successfully designed and prototyped. It was proven that this robot addressed all design requirements for a duct travelling mobile robot. This novel design proved to have capabilities not found in just one robot. There are robot designs for vertical climbing, designs for facilitating turns to the right and left, and designs that focus on speed and efficiency of mobility, but very few robot designs group all these requirements into a single structure like the wheeled tensegrity mobile robot does.

This research furthers the knowledge in the ever-growing field of tensegrity mobile robotics. It actually opens a new sub-category of hybrid wheeled-tensegrity mobile robotics. The project methodology was proven successful as it led to an optimised design that fulfilled all requirements. It had an advantage over simulation and analytical methods in these particular circumstances. It certainly was best to approach the research by broadly study structures and build models to assess their properties. The criteria of evaluation were validated by prototyping. Accepted designs by the criteria were stable. Rejected designs by the criteria were unstable. Furthermore, these criteria need to be expanded. The author sees many more possibilities of growth that were not pursued due to time constraints. Tensegrity robots do not need to address all design requirements with a tensegrity solution. Hybrid approaches have just been proved to be valid. Practical applications should start to appear more in research work. Transition areas should not be constrained to mobile robotics. They can be applied to add tensegrity structures to many other fixed structures.

Future work could include computer simulation to refine the topology created, building a prototype with metal springs and a metal body, possibly aluminium, adding motorised actuators to control the structure. Flexinol was also tested on this prototype as actuator but the amount of actuation was much smaller than the structure required. Future work could also include Flexinol as actuator in a pulley arrangement. Future work could also include exploring other topologies applied to wheeled tensegrity robotics and keep developing the criteria and designs for soft transitional regions.

Declarations

Acknowledgements

For their support, we thank the DMEM lab technicians including Dino Bertolaccini, Duncan Lindsay, and Jim Mitchell. Many thanks also go to Tom Flemons for sharing the wisdom of many years building tensegrity structures.

Authors' Contributions

Mr. Carreño performed the formal literature review, built the tensegrity structures, designed and constructed the wheeled tensegrity mobile robot prototype, performed the laboratory evaluation of materials and mobility, and wrote the paper. Dr. Post researched and presented the concept for a wheeled tensegrity robot, assembled the literature, supervised the work, and co-wrote the paper.

Competing Interests

The authors declare that they have no competing interests.

Funding

This research was supported by internal funds from the Department of Design, Manufacture, and Engineering Management at the University of Strathclyde, and by provision by the Department of laboratory resources, materials for prototype construction, and expertise on the part of the laboratory technicians in constructing the prototypes.

References

- [1] Gough, M. (1998). In the Laboratory of Constructivism: Karl Ioganson's Cold Structures. *October*, 84: 91-117. doi:10.2307/779210
- [2] Snelson, K. (1990). Letter from Kenneth Snelson to R. Motro. *International Journal of Space Structures*. [online] Available at: <http://www.grunch.net/snelson/rmoto.html> [Accessed 19 Jul. 2017]
- [3] Grimes, W. (2016). *Kenneth Snelson, Sculptor Who Fused Art, Science and Engineering, Dies at 89*. [online] The New York Times. Available at: <https://www.nytimes.com/2016/12/23/arts/design/kenneth-snelson-dead-sculptor.html?smid=tw-nybits&smtyp=cur> [Accessed 25 Jul. 2017].
- [4] Hernández, S. & Mirats, J. (2009). Tensegrity frameworks: Static analysis review. *Mechanism and Machine Theory*, 43(7): 859-881.
- [5] Skelton, R. E., Adhikari, R., Pinaud, J. -P., Chan, W. L., & Helton, J. W. (2001). An Introduction to the Mechanics of Tensegrity Structures. *IEEE Conference on Decision and Control*. 5: 4254-4259.
- [6] Komendera, E. (2012). A Survey of the Computational Modeling and Control of Tensegrity Robots.
- [7] Chen, Y., Feng, J. & Wu, Y. (2012). Novel Form-Findind of Tensegrity Structures Using Ant Colony Systems. *Journal of Mechanisms and Robotics*. 4: 1-7.
- [8] Rieffel, J., Trimmer, B. & Lipson, H. (2008). Mechanism as mind: What tensegrities and caterpillars can teach us about soft robotics. *Artificial Life XI: Proceedings of the 11th International Conference on the Simulation and Synthesis of Living Systems, ALIFE 2008, 2008*: 506-512
- [9] Williamson, D. & Skelton, R.E. (2003). General Class of tensegrity Structures: Topology and Prestress Equilibrium Analysis. *Journal of guidance, control, and dynamics*. 26(5): 685-694.
- [10] Motro, R. (2009). Structural morphology of tensegrity systems. *Asian Journal of Civil Engineering Building and Housing*. 10 (1): 1-19.
- [11] Rieffel, J., Valero-Cuevas, F., & Lipson, H. (2009). Automated Discovery and Optimization of Large Irregular Tensegrity Structures. *Computers and Structures*. 87: 368-379.
- [12] Hernández, S. & Mirats, J. (2008). A Method to Generate Stable, Collision Free Configurations for Tensegrity Based Robots. *IEEE/RSJ International Conference on Intelligent Robots and Systems*. 3769-3774.
- [13] Micheletti, A. & Williams, W.O. (2007). A Marching Procedure for Form-Findind for Tensegrity Structures. *Journal of Mechanics of Materials and Structures*. 2(5): 857-882.
- [14] Levin, S. (2002). The Tensegrity-Truss as a Model for Spine Mechanics: Biotensegrity. *Journal of Mechanics in Medicine and Biology*. 02(03&04): 375-388.
- [15] Tietz, B. R., Carnahan, R. W., Bachmann, R. J., Quinn, R. D, SunSpiral, V. (2013). Tetraspine: Robust Terrain Handling on a Tensegrity Robot using Central Patter Generators. *2013 IEEE/ASME International Conference on Advanced Intelligent Mechatronics (AIM) Wollongong, Australia*. 261-267.

- [16] Mirletz, B.T., Park, I. –W., Flemons, T. E., SunSpiral, V. (2014). Design and Control of Modular Spine-Like Tensegrity Structures. *6th World Conference of the International Association on Structural Control and Monitoring*.
- [17] Sabelhaus, A. P., Ji, H., Hylton, P., Madaan, Y., Yang, C. W., Agogino, A. M., Friesen, J., SunSpiral, V. (2015). Mechanism Design and Simulation of the ULTRA Spine: A Tensegrity Robot. *Volume 5A: 39th Mechanisms and Robotics Conference*.
- [18] Hustig, D. SunSpiral, V., Teodorescu, M. (2016). Morphological Design for Controlled Tensegrity Quadruped Locomotion. *2016 IEEE/RSJ International Conference on Intelligent Robots and Systems (IROS)*. 4714-4719.
- [19] Scarr, G. (2012). A consideration of the elbow as a tensegrity structure. *International Journal of Osteopathic Medicine*. 15(2): 53-65.
- [20] Lessard, S., Bruce, J., Jung, E., Tedorescu, M., SunSpiral, V., Agogino, A. (2016). A lightweight, multi-axis compliant tensegrity joint. *IEEE International Conference on Robotics and Automation (ICRA)*. 630-635.
- [21] Bliss, T., Iwasaki, T. and Bart-Smith, H. (2013). Central Pattern Generator Control of a Tensegrity Swimmer. *IEEE/ASME Transactions on Mechatronics*, 18(2): 586-597.
- [22] Motro, R., Najari, S. & Jouanna, P. (1987). Static and Dynamic Analysis of Tensegrity Systems. *Lecture Notes in Engineering*. 270-279.
- [23] Mirats-Tur, J.M., Hernández, S. & Rovira, A. G. (2007). Dynamic Equations of Motion for a 3-bar Tensegrity Based Mobile Robot. *IEEE International Conference on Emerging Technologies and Factory Automation, ETFA*. 1334-1339.
- [24] Cefalo, M. & Mirats-Tur, J.M. (2011). A comprehensive dynamic model for class-1 tensegrity systems based on quaternions. *International Journal of Solids and Structures*. 48: 785-802.
- [25] Skelton, R. & Oliveira, M. (2009). *Tensegrity Systems*. Springer.
- [26] Friesen, J. M., Glick, P., Fanton, M., Manovi, P., Xydes, A., Bewley, T., SunSpiral, V. (2016). The Second Generation Prototype of A Duct Climbing Tensegrity Robot, DuCTTv2. *2016 IEEE International Conference on Robotics and Automation (ICRA)*. 2123-2128.
- [27] Paul, C., Roberts, J. W., Lipson, H., Cuevas, F. C. (2005) Gait Production in a Tensegrity Based Robot. *Advanced Robotics, 2005. ICAR '05. Proceedings*.
- [28] Rovira, A.G. & Mirats-Tur, J.M. (2009). Control and simulation of a tensegrity-based mobile robot. *Robotics and Autonomous Systems*. 57(5): 526-535.
- [29] Shibata, M., Saijyo, F., Hirai, F. (2009). Crawling by Body Deformation of Tensegrity Structure Robots. *IEEE International Conference on Robotics and Automation*. 4375-4380.
- [30] Bruce, J. Sabelhaus, A. P., Chen, Y. X., Lu, D. Z., Morse, K., Milam, S., Caluwaerts, K., Agogino, A. M., SunSpiral, V., Cruz, S. (2014). SUPERball: Exploring Tensegrities for Planetary Probes. *12th International Symposium of Artificial Intelligence, Robotics and Automation in Space (i-SAIRAS)*.
- [31] Sabelhaus, A. P., Bruce, J., Caluwaerts, K., Manovi, P., Firoozi, R. F., Dobi, S., Agogino, A. M., SunSpiral, V. (2015). System Design and Locomotion of SUPERball, an Untethered Tensegrity Robot. *2015 IEEE International Conference on Robotics and Automation (ICRA)*.
- [32] Friesen, J. Pogue, A., Bewley, T., De Olieria, M., Skelton, R., & SunSpiral, V. (2014). DuCTT: a Tensegrity Robot for Exploring Duct Systems. *IEEE International Conference on Robotics & Automation (ICRA)*. 4222-4228.
- [33] SunSpiral, V. Gorospe, G., Bruce, J., Iscen, A., Korbel, G., Milan, S., Agogino, A., & Atkinson, D. (2013). Tensegrity Based Probes for Planetary Exploration: Entry, Descent, and Landing (EDL) and Surface Mobility Analysis. *International Journal of Planetary Probes*. 7.
- [34] Flemons, T., Tensegrity Robot with Wheeled Locomotion 2017.
- [35] Complete Anatomy. (2017). Software App. Dublin: 3D4Medical Ltd.

- [36] Motro, R. (1992). Tensegrity Systems: The State of the Art. *Journal of Space Structures*. 7(2): 75-83.
- [37] Schuenke, M., Schulte, E., & Schumacher, U. (2010) Thieme *Atlas of Anatomy: General Anatomy and Musculoskeletal System*. New York: Thieme.